32nd Congress of the International Council of the Aeronautical Sciences
September 6-10, 2021
Pudong Shangri-La, Shanghai, China

IMPLEMENTATION OF DISTRIBUTED ELECTRIC PROPULSION ON A GENERAL AVIATION AIRCRAFT

Murilo A. Gallani[1], Luiz Carlos S. Góes[2] & Luiz Augusto R. Nerosky[3]

[1]Instituto Tecnológico de Aeronáutica - ITA
[2]Instituto Tecnológico de Aeronáutica - ITA
[3]Embraer S.A.

Abstract

With an always increasing demand for more efficient aircraft due to both economic and environmental purposes, academy and industry are studying hybrid-electric and full-electric concepts to explore new aircraft design opportunities. This paper expands on the results of previous publications, using a Cessna 208B Grand Caravan as a platform for the implementation of distributed electric propulsion to enable the use of high-lift propellers. The design space is swept to evaluate the impacts of the technology in wing weight, propulsive system sizing and weight as well as in payload, range and fuel consumption on different simulated missions. The models are integrated using SUAVE, a conceptual level design environment, which is used to integrate the aircraft model and run the simulations. Results show that generating enough extra lift with the propellers require large amounts of power, resulting in a heavy propulsive system that hinders the payload and range capabilities of the aircraft and are unfortunately not compensated by the small aerodynamic gains generated by this configuration.

Keywords: Distributed Electric Propulsion, High Lift Propellers, Conceptual Design, Hybrid Electric Propulsion, Simulation

1. Introduction

Electrification has been a growing topic of interest in the aeronautical industry, which has been researching and investing on a number of new concepts and technologies in search of reductions in fuel burn and emissions on the atmosphere [1,2]. Recent studies show, however, that unless very optimistic technology assumptions are used, specially on the battery side [3], electrifying or hybridizing conventional aircraft propulsion do not easily bring clear benefits [4–6].

The most interesting option is to use electrification as a way to seek positive, advantageous interactions between propulsors and airframe to increase flight efficiency with aircraft-propulsion integration [7]. The usage of electric energy to distribute power across the aircraft along with the great scalability of electric machinery and power electronics allows electrification to be used to explore new engine mount positions, distribute propulsors along the wing, empennage or fuselage and even to try out new fuselage and wing forms and configurations in the search for positive aircraft-propulsion interactions and better efficiency.

With this in mind, this paper expands on previously presented analyses [8] on the efficiency gains of Distributed Electric Propulsion (DEP) when used to enable the installation of High-Lift Propellers (HLP) along the wing to increase the wing's maximum lift coefficient, allowing for wing reduction and gains in aerodynamic efficiency. Using a model Cessna 208B Grand Caravan as reference and modifying it to accommodate the DEP technology, this paper shows a design space exploration of key variables to observe the impacts on wing weight and propulsive system sizing and weight. After choosing a design point the models are then run on different missions to observe the operation of the propulsive system and compare the fuel consumption of both conventional and DEP aircraft.

1.1 Literature review

Distributed Electric Propulsion tries to take advantage of the interaction between propulsors and the airframe in many different ways to bring benefits to the aircraft, one of them being the use of High Lift Propellers which has been explored in many different publications [9–13]. This concept uses a number of relatively small propellers positioned along a large portion of the leading edge of the wing, using them to accelerate the airflow on the wing increasing the dynamic pressure and generated lift. An example of this concept can be seen in Figure 1. Concepts that use this technology usually propose to use the high lift propellers only at low speed flight, complementing the flaps when higher values of lift coefficient are needed, while at higher speed the blades are folded back and thrust is generated by more conventional propellers.

The HLP increases the maximum lift coefficient of the wing which allows the aircraft, when compared to a conventional one, to fulfill stall speed or field length requirements with a smaller wing area and higher wing loading. Publications on this concept propose that this can bring the aircraft to cruise at or near its optimal C_L, when the aerodynamic efficiency for its drag polar is at it's peak, bringing large overall efficiency gains [12, 13].

Other studies try to quantify the advantages and feasibility of such configuration. With a concept aircraft similar in size to the Cirrus SR22, Stoll *et al.* [9] achieves an L/D of over 20 by using high-lift propellers to increase the $C_{L_{max}}$ from 3.4 to 5.2 and reduce the wing area by 62%. Following this work, Stoll [10] compares experimental data with CFD simulations showing, based on preliminary results, that the desired C_{Lmax} for the project may actually be exceeded.

Figure 1 – A concept aircraft using the HLP technology. [9]

Recent publications have also tackled this subject but achieved less optimistic results. Gallani *et. al* [8] integrates many different models in a drag build up method along with HLP and lift augmentation surrogate models to evaluate the gains of this technology on a Cessna 208B Grand Caravan in a partial-turboelectric configuration. According to the theory used in previous publications, this aircraft could theoretically achieve up to a 23% increase in cruise L/D if the wing area is reduced by half.

The authors do an extensive exploration of the design space, varying wing area and dynamic pressure increase by the high lift propellers and calculating the aircraft drag through the build up methods, including the drag from the newly added nacelles for the electric motors on the wings. Two strategies for wing area reduction are used, those being constant-wingspan and constant-aspect ratio. The results show that the best option is the constant wingspan one as the induced drag remains the same as the wing area is reduced, whereas on the second strategy the induced drag is increased. As for parasitic drag, it is reduced in both strategies following the reduction of wetted area.

This is however not enough to achieve the gains proposed by the previous theory, reaching a L/D increase of only 4% even if some operational limitations exposed by the study are ignored. It shows that even if the extra nacelle drag is also ignored the best aerodynamic efficiency increase that can be achieved is around 8.5%, still way short of the 23% that the previous theory proposes. The conclusion is that this difference is due to an assumption used on the previously cited papers that keep a constant drag polar when evaluating the efficiency changes of the wing reduction, which is not true because as the wing area changes the drag polar must change as well. To keep the polar constant means that drag of the whole aircraft is being reduced along with the wing area, while in fact the only thing that changes is the parasitic drag on the wings.

2. Models

To analyze the effects of high-lift propellers on the weight and operation of an aircraft a few core models were integrated on the Stanford University Aerospace Vehicle Environment (SUAVE) [14]. This is a tool that will work as a mission solver to generate the results for the analyses and was made specifically for conceptual level design to study unconventional and futuristic aircraft. The most relevant models for this paper will be briefly explained in this section, however more information can be found if desired on other publications [8, 15].

2.1 Reference aircraft and engine

The Cessna 208B Grand Caravan baseline model was made by estimating the original aircraft drag polar and then calibrating an aircraft model on SUAVE to match its performance. The estimation process used cruise flight data from the Grand Caravan Information Manual [16] to get a polar of $C_D = 0.03689 + 0.04606\, C_L^2$. The drag from this polar is then incremented, when needed, by flap drag and other effects.

The thermal engine was modeled on a similar manner, gathering power, torque and fuel flow data from the Manual to build a model that represents its fuel consumption throughout the mission. Figure 2a shows the power ratio from the engine for various values of air density ratio, the first one being the ratio between the available power at full throttle and the engine rated power, and the second the ratio between the local air density and the air density at sea level on a standard atmosphere. The engine behavior is almost exactly the same for 1750 and 1900 RPM, but differs for 1600 RPM. This last set of data was ignored for the model and the engine in this study will only operate above 1750 RPM.

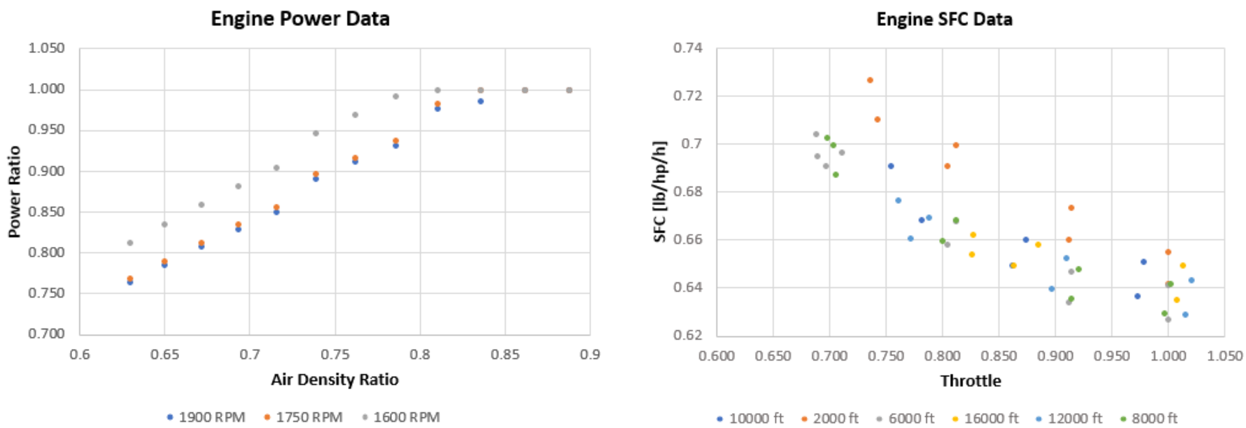

(a) Engine power data.

(b) Engine SFC data.

Figure 2 – Grand Caravan engine data.

$$P_{ratio} = 1.15205\,\sigma + 0.03715 \tag{1}$$

$$SFC = SFC_{nom}\left(0.6868\,\Pi^2 - 1.4843\,\Pi + 1.7975\right) \tag{2}$$

Other effect that is important to be captured by the model is the fuel consumption at different throttle lever positions, the throttle lever representing the ratio between shaft power and available power. Figure 2b shows the data gathered for different conditions, including different altitudes, but all the points were used together for an unified model for all altitudes. Equations 1 and 2 show the final model used on this study with P_{ratio} and σ being the available power and air density ratios, SFC

the resulting specific fuel consumption, Π the throttle lever, and SFC_{nom} the nominal SFC which was calibrated to 0.653 to better match Manual data on climb and cruise fuel consumption. On Equation 1 the result is capped at one so that the model does not yield more power than the engine is rated for.

2.2 Hybrid-electric aircraft model

The modified hybrid-electric aircraft uses as a starting point the previously modeled Grand Caravan so the model is in large part unaltered, except for the propulsive system and wing changes.
The chosen propulsive architecture is a partial-turboelectric, as seen on Figure 3. On this system the turboprop engine remains exactly where it is on the conventional aircraft, powering the cruise propeller mechanically through a gearbox. Connected on the same shaft that powers the propeller is a generator, so that the total shaft power delivered by the engine can be properly split between both components. The power supplied by the generator is distributed to the electric motors that drive the high-lift propellers through cables and motor controllers. The motors are installed on nacelles that are exposed to the airflow, so their drag is estimated and included in the performance of the aircraft. This architecture was chosen was to minimize the impact in propulsive efficiency during cruise, since it is usually the longest flight phase and consumes a lot of energy. By maintaining the original engine-propeller mechanical coupling during cruise no electrical losses take place, maximizing efficiency during this flight phase. On the electrical side, the choice for a generator instead of a battery system was mainly due to the high weight of batteries due to low specific power and energy.
Given the heat dissipated by these components a liquid cooling system to cool down the motors and controllers was considered on both weight and drag estimations as well.

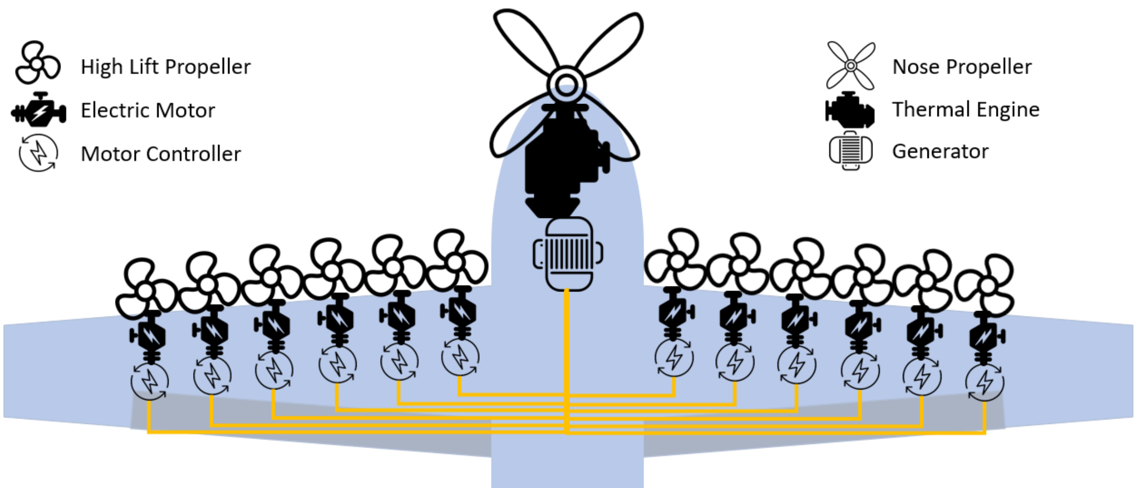

Figure 3 – Chosen propulsive architecture.

The drag estimation methods include the wing parasitic and induced drag as well as the parasitic drag from the nacelles of the electric motors on the wing so that the changes in wing and motor size properly affect the aircraft performance.

2.3 Propellers

There are two different types of propellers on this study with very different characteristics. The nose propeller, present both on the conventional and on the hybrid-electric aircraft, is a conventional, variable pitch propeller that is responsible for generating thrust throughout all the flight phases. For this one the model used was the default SUAVE model that evaluates thrust and power based on blade element theory for a geometry that is created based on a set design point [14] .
The ones on the wing are very different as they are fixed pitch propellers designed to operate only at low speeds while generating a strong slipstream to increase dynamic pressure on the wing. The main thing to be modeled for the HLP is the relationship between propeller size, thrust, slipstream velocity and power to size the motors. The chosen method to model these propellers was the momentum theory, represented by Equations 3 and 4. They allow for the calculation of the generated thrust T or

slipstream velocity v_i based on propeller disk area A, freestream velocity V_∞ and air density ρ without worrying with details of the propeller geometry.

$$T = \rho A \left(V_\infty + v_i\right) \left(2 v_i\right) \tag{3}$$

$$v_i = \frac{-V_\infty + \sqrt{V_\infty^2 + \frac{2T}{\rho A}}}{2} \tag{4}$$

To estimate propeller efficiency data from a high-lift propeller data from design exploration made by Patterson [13] was used and, on the design point with an advance ratio of 0.65, was around 64%. On off-design operation, the propeller performance was evaluated with thrust and power coefficient curves as function of advance ratio, seen on Figure 4, that were generated based on the available data. The polynomials for the thrust coefficient C_t and power coefficient C_p as function of advance ratio J are seen on Equations 5 and 6 respectively. The high values of efficiency seen are due to the fact that the airframe and nacelle effects on the propeller, which reduces efficiency, are not taken into account on the model.

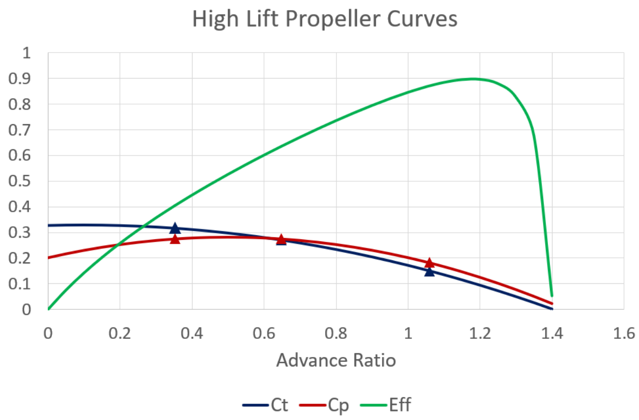

Figure 4 – High-Lift Propellers performance data.

$$C_t = -0.193\,J^2 + 0.0374\,J + 0.3268 \tag{5}$$

$$C_p = -0.3214\,J^2 + 0.322\,J + 0.2021 \tag{6}$$

2.4 Wing weight

The wing is the only part of the original aircraft that will be subject to changes so the model presented by Stoll and Mikic [11] to estimate wing weight for this kind of aircraft was used. It takes into account many geometric characteristics of the wing such as area, wetted area, thickness, aspect ratio and sweep, as well as material characteristics like density and allowable stress. It is worth noting as well that this model does not take into account the installation and distribution of multiple motors, which may result in the weight estimates being actually a little optimistic.

2.5 Electric machines

The generator and motor are both electrical machines and so, despite their constructive differences, share the same performance and weight models in this study.

The performance model evaluates the efficiency of the machines depending on the shaft torque and angular speed, approximating the behavior of real machines. They are completely scalable to any power rating and are calibrated differently for motors and generator to replicate the differences in the machines.

The weight model goes a little bit further than the traditional specific power estimates that are broadly used in different studies, taking into account not only the motor power but also it's nominal angular speed on the weight estimate . This adds another level of sensitivity to the analyses since the effects of using different sized propellers that operate at different speeds will be captured on the weight of the machines through this model.

The motor general dimensions, specially its cross section, are very important for this work because larger motors will generate more nacelle drag counteracting the benefits of the DEP. Like the weight model, the volume model captures variations of length and diameter with nominal power and rated speed.

3. Design space exploration

This section presents the results from the design space exploration, where two variables are swept over a range of values and the effects on the aircraft design are observed.

One of the main components to be changed and observed is the wing. Simplifications were made to reduce the number of variables to be watched and to remove effects that are not related with the wing blowing effect as described on [15], resulting in the first variable of the design space exploration which is wing area ratio. The S_{ratio} represents the ratio between the wing area of the subject under evaluation and the original Grand Caravan wing area.

Given the results obtained and presented on [8] this paper focuses on the constant-wingspan strategy, meaning that the reduction of wing area will be through reduction of chord, keeping the wingspan constant and increasing aspect ratio. Since drag calculation evaluates each component's drag individually, the changes in wing will affect the drag and performance of the aircraft.

The second quantity to be varied and observed is the dynamic pressure ratio imposed by the high-lift propellers by its accelerated slipstream. The q_{ratio} represents the ratio between the dynamic pressure on the wing, behind the slipstream of the propellers, and on the undisturbed flow, which is what increases lift generation and the wing $C_{L_{max}}$, allowing the wing area reduction.

One important result that will be used in this paper is that despite exploring many values of q_{ratio} for each value of S_{ratio} there is a minimum feasible value that, given the lift augmentation results from the implemented models, can increase the the $C_{L_{max}}$ enough so that the stall speed of the original aircraft remains unchanged at 61 kt [8].

3.1 Sizing process

The wing chord and area are direct outputs of the chosen S_{ratio} for each evaluated subject, so this step is very straightforward. The motor sizing, however, requires more explanation.

It starts with the propeller diameter, which is defined by the number of propellers on the wing and the span where they are installed. To simplify the evaluations it was defined that the propellers would always be installed on the same span as the flaps, which goes from the wing root to almost the tip but not does not cover it entirely. This is in line with the lift augmentation model from Patterson [13], who states that its accuracy is compromised near the wingtip due to the three-dimensional nature of the flow. For the initial design space exploration a total of ten propellers were used but further on this section a study on the effects of the propeller number will be presented.

The desired q_{ratio} directly yields, based on the dynamic pressure of the undisturbed flow at the design point (stall speed of 61 kt) the required speed of the propeller slipstream. Given the propeller diameter (and thus disk area), Equation 3 is used to evaluate the required thrust and, based on the efficiency model from Figure 4 and an advance ratio for a design tipspeed of 137 m/s, its required power. Since this thrust and power might not match the thrust and power coefficient data used for the model, a scaling factor is calculated to evaluate the thrust and power at different operating points with the polynomials from Equations 5 and 6.

This required power for the propeller is the same for the motor, and given the propeller RPM calculated by its tipspeed and diameter, the design motor RPM is also defined. Considering the motor and controller efficiencies and the number of propellers, the power requirements for the whole electrical system are set.

3.2 Thrust and power

The byproduct of lift augmentation through increasing dynamic pressure is the generation of thrust. Figure 5a reproduces previous results where the red line shows the required thrust from the HLP to generate the minimum required q_{ratio} to keep the aircraft from stalling at different values of S_{ratio} [8]. The blue line shows the total thrust required by the aircraft to keep flying at the stall speed of 61 kt. For S_{ratio} values above 0.8 the designs are clearly feasible, since the HLP supply part of the required thrust and the rest can be supplied by the cruise propeller.

For lower values, however, there is a complication because the high-lift propellers generate more thrust than the required to maintain flight. This at first may not seem like a problem but it means that the aircraft would never be able to decelerate to lower speeds if needed, such as for touchdown. It also means that to fly at this speed the HLP would have to generate less thrust, reducing the lift and stalling the aircraft, meaning that the effective stall speed for such designs are actually higher than the desired 61 kt.

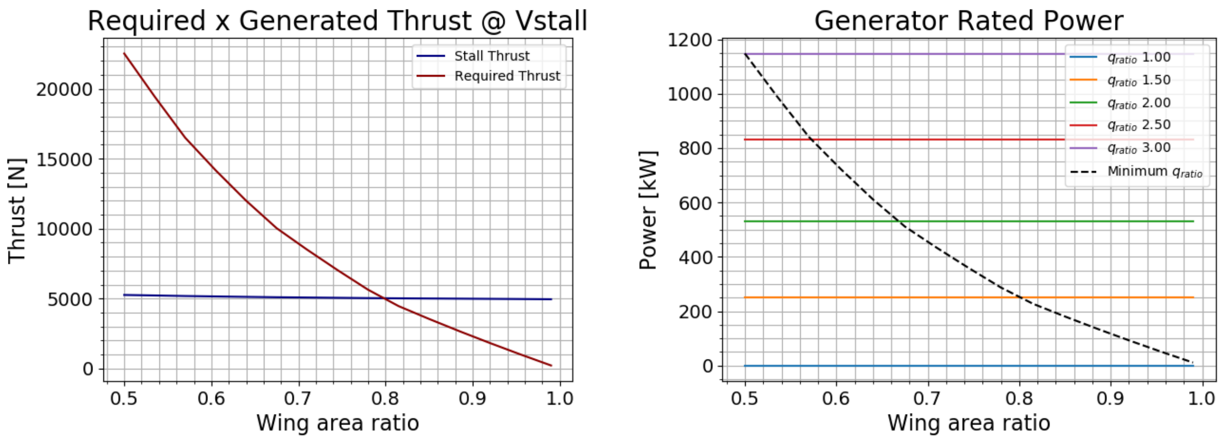

(a) Thrust data. [8]

(b) Generator power data.

Figure 5 – Thrust and Power across the design space.

The required power rating of the generator, which must supply electricity to all of the motors plus the system losses, can be seen on Figure 5b. The colored lines show the power rating for different values of q_{ratio} while the black dotted lines represents the power rating for the minimum q_{ratio}, as explained earlier.

As expected, smaller wings require higher increases of dynamic pressure, which in turn require more power and bigger generators. A point of attention is that the Grand Caravan engine power rating is approximately 500 kW, so power requirements of more than that would require an increase of engine size or the addition of batteries as an auxiliary power source. However, this only becomes an issue when the wing area ratio is around 0.68 or less, meaning that for this aircraft the previous thrust restrictions are more severe.

These results limit the design space by quite a lot, specially the elevated thrust generation. It may be possible to achieve wing area ratios a little smaller than the limits found by increasing drag through new mechanisms on the aircraft like fuselage spoilers, or by adjusting the cruise propeller to create drag and using the generator to direct some of that power to the high-lift propellers. It seems however that large area reductions to decrease drag are highly unlikely.

3.3 Weight

The weight effects on the aircraft can be summed up into wing and propulsive system weight variations, since the maximum take-off weight of the aircraft on this study remains the same and other components such as fuselage or stabilizers are unchanged.

The wing weight, shown in Figure 6a, increases significantly with the area reduction because the weight model is sensitive to both span and aspect ratio. With a constant wingspan the aspect ratio increases as the area reduces and so does the weight. It is important to notice that this model is not sensitive to number, size or weight of the wing motors, so this is something that is not shown in this figure.

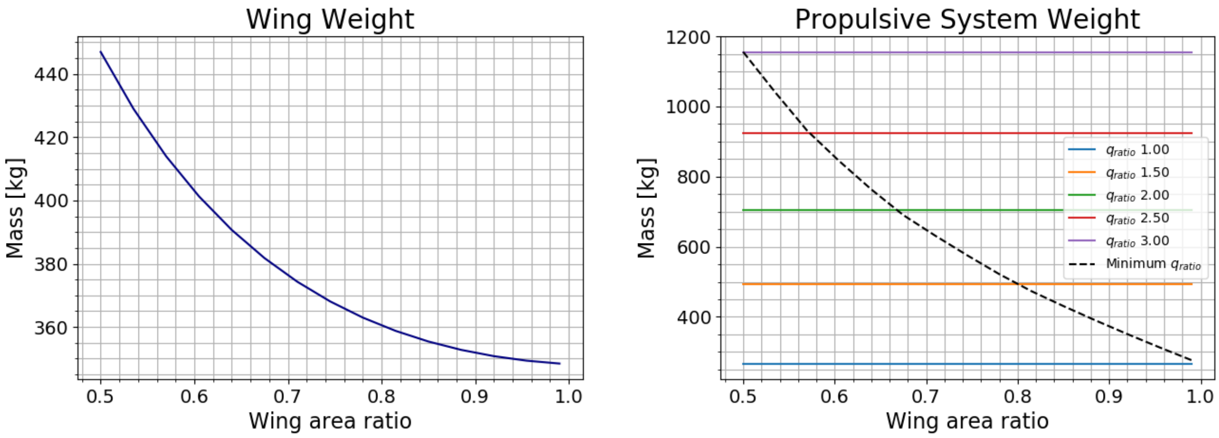

(a) Wing weight.

(b) Propulsive system weight.

Figure 6 – Weight variation.

As for the propulsive system weight, the trends follow closely those presented before regarding component power, as power and weight are closely related on all propulsive components. Figure 6b shows in the colored lines the weight for different q_{ratio} values and the black dotted lines represent the actual weight for the minimum feasible design.
Since the MTOW is unchanged any weight change must be reflected on either payload or fuel weight, to be defined depending on which would be less detrimental to the operation. Due to the increase in both wing and propulsive system weight the aircraft mission is expected to be greatly impacted by the use of this technology, possibly compromising the aerodynamic gains that comes with it.

3.4 Effects of the number of propulsors

The number of chosen propulsors for the lift augmentation is expected to have some effect on the results, so all the analyses were repeated with this number varying from 8 to 16 motors. This number directly effects the propellers diameter, reducing it as the number increases.

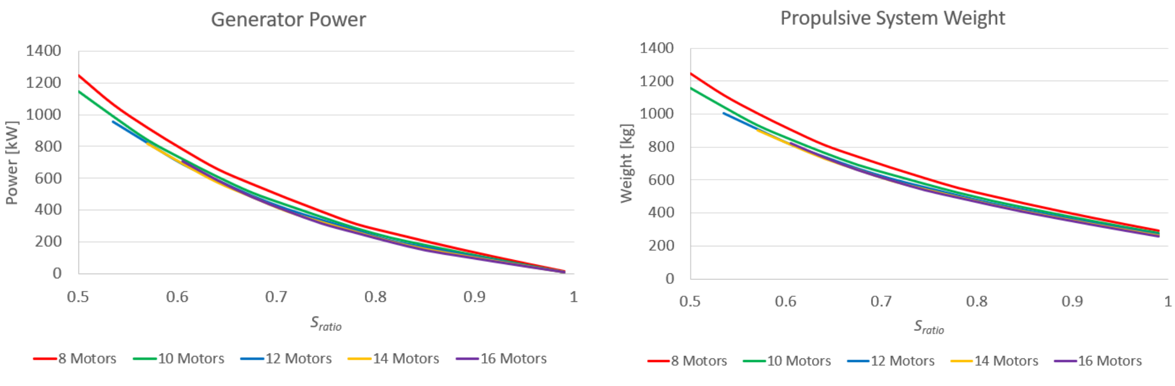

(a) Generator power.

(b) Propulsive system weight

Figure 7 – Installed electric power and system weight.

A reduction in propeller diameter brings benefits such as higher induced velocity (and dynamic pressure ratio) for the same amount of thrust, and higher RPM values for the same tipspeed which may bring weight reduction to the motors. This is, however, somewhat counteracted by the fact that the propellers disk dimensions are very close to the wing chord, requiring more dynamic pressure for a given lift increase [13].
The results are shown in Figure 7 where both Generator Power and Propulsive System Weight are shown. These figures show that a higher number of motor is in fact slightly beneficial in terms of installed power and weight, but there is not much improvement past 10 or 12 motors.

4. Mission analyses

After seeing how the design space is shaped and limited the next step is to select one design point, size the aircraft and compare its performance with the baseline Cessna Grand Caravan, focusing on the operation of the system and the impacts on the range/payload and fuel consumption of the aircraft. The operation of the high-lift propellers is controlled by an extra variable called electric throttle. This variable controls the RPM of the electric motors which in turn will affect the generated thrust and $C_{L_{max}}$ of the aircraft according to the implemented models.

As for the mission, a couple of different ones will be set up for the analyses depending on the desired aspects to be checked. A main climb-cruise-descent will be set up for the mission, but other segments will be added to better represent a typical Caravan Mission and show the segments right after takeoff and landing, where the DEP system is actually powered on. These segments will be called Climb-out and Approach and actually consist of a number of SUAVE segments to represent different stages of flight that are presented on the Grand Caravan Information Manual. A 45 minutes alternate mission will also be added for considerations regarding fuel reserves for the aircraft.

4.1 Design Point

The design point is a combination of wing area, design dynamic pressure increase and number of high lift propellers. Given the previous results the chosen number of propulsors for these analysis was 12, with a wing area ratio of 0.72. This number should push the design slightly into the region where the HLP thrust at the design point is larger than the required thrust to keep flying at the stall speed. It is assumed that an extra 2000 *N* of drag can be generated by the nose propeller by operating it in a windmilling condition to compensate for this. The chosen design point and resulting aircraft data can be seen on Table 1, along with the conventional aircraft data for reference. According to the results from Gallani *et. al* [8] this wing reduction of 28% should yield efficiency gains on the order of 3%.

	Conventional	DEP
Design q_{ratio}	-	1.8
Design S_{ratio}	-	0.72
Wing Area [m2]	25.96	18.69
Wingspan [m]	15.88	15.88
Aspect Ratio	9.71	13.48
Mean Aerodynamic Chord [m]	1.64	1.18
Wing Weight [kg]	348.3	372.42
Propusive System Weight [kg]	214.5	559.1
HLP Radius [cm]	-	40.33
Nacelle Radius [cm]	-	10.26
Electric Motor Power [kW]	-	26.0
Generator Power [kW]	-	345.5

Table 1 – Summary of the reference and modified aircraft

The added weight for the new wing and new propulsive system raises the empty weight of the aircraft by almost 370 *kg*, which represents a significant drop in either fuel weight, payload or both. A breakdown of the propulsive system details can be seen on Table 2 for better understanding of which components contribute the most for this weight increase. Note that in this table the “rated power” for the cooling system represents the heat load that must be cooled. It can be seen that a good opportunity of weight savings would be to take credit of the flow over the nacelles to cool down the motors and power electronics, thus avoiding a heavy cooling system.

These numbers show specific powers of 4 and 5.2 kW/kg for the generator and electric motors, which seems on par with the current state of the technologies for these machines. The motor controllers specific power, however, is at only 3.6 kW/kg which is way too low. This indicates that the used model for these components might be badly calibrated for this power rating and a revision is needed. The same goes for the cabling weight, which seems very optimistic at less than 4 kg, although this may be a result from the relatively low power of each individual controller and the high voltage (600V) used.

Component	Rated Power [kW]	Weight [kg]	Diameter [m]
Engine	503.0	160.0	-
Cruise Propeller	-	54.5	2.69
Generator	345.5	85.8	-
Cabling	-	3.9	-
Controllers (each)	27.4	7.4	-
Electric Motors (each)	26.0	5.0	0.19
High Lift Propellers (each)	-	5.0	0.81
Cooling	32.0	45.7	-

Table 2 – Propulsive System breakdown.

4.2 Critical Points

The wing area reduction applied results in the need of the high lift propellers to operate at low speeds to increase the maximum C_L of the aircraft and keep it from stalling. It is thus very important to verify if the lift increase requirements are being met on the critical parts of the mission, namely the Climb-out and Approach segments where the speeds are lower and the smaller wing would stall.

Figure 8 – Critical points mission profile.

For that goal a mission containing three Climb-out, a Descent and the three Approach portions of the mission was simulated, with the aircraft flying at its MTOW, as shown in Figure 8. The electric throttle is at 100% during the first Climb-out segment, 80% at the second segment, and 70% on the last approach segment. On the rest of the mission the electric motors are turned off.

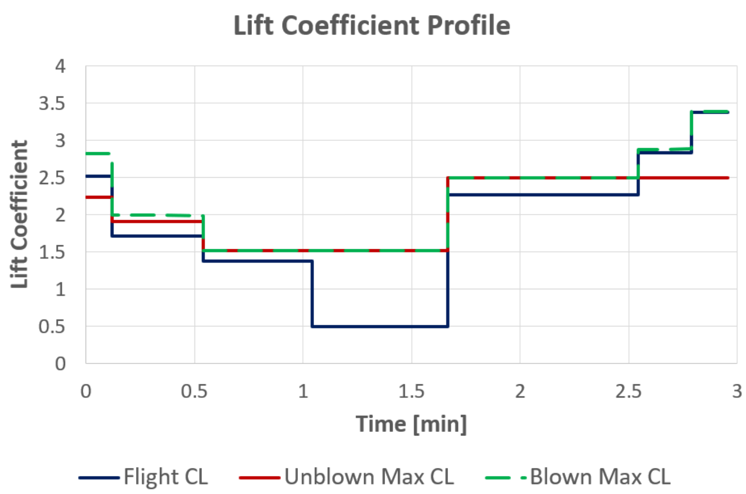

Figure 9 – C_L at critical conditions.

Figure 9 shows the unblown maximum lift coefficient, blown maximum lift coefficient and the flight lift coefficient. It can be seen that for the first Climb-out and the last two Approach segments the lift augmentation is really needed as the aircraft is flying at such low speeds that the flight C_L is higher than the unblown maximum C_L achieved only with flaps while on the other segments the conventional high-lift system is enough to keep the aircraft from stalling.
Another interesting point to look at is how the propulsive system is operating under these conditions. Figure 10 shows the thrust generated by the cruise propeller and the high lift propellers in comparison with the total thrust generated on the same mission by the conventional aircraft. For the first Climb-out segment the high lift propellers are at full throttle, generating almost 6000 N of thrust while the nose propeller is operating with much less thrust. On the second segment this situation changes as the RPM of the HLP is dialed back, causing it to generate less thrust and less lift increase.

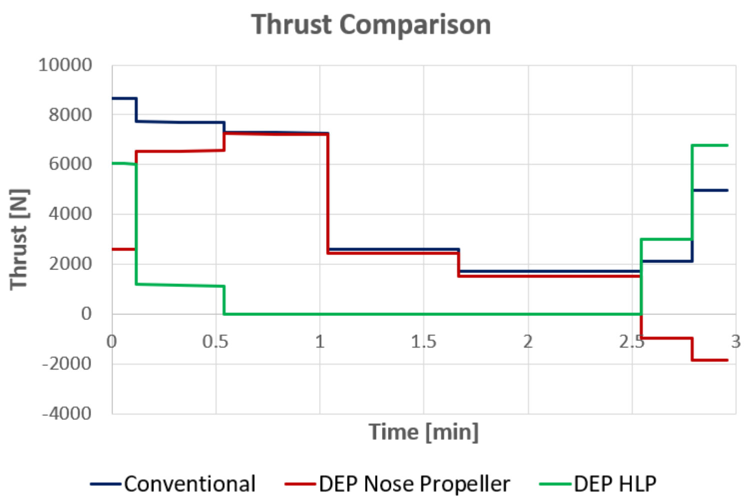

Figure 10 – Thrust at critical conditions.

On the next segments the HLP are turned off as there is no need for lift augmentation and are turned back on the last two Approach segments. Here comes the foreshadowed condition where the nose propeller needs to generate drag so that the aircraft can achieve the desired sink rate. For the lift augmentation the HLP are generating so much thrust that the nose propeller has to create almost 2000 N of extra drag on the last segment, which is when the aircraft is flying at its stall speed. Unfortunately this condition is very close to the windmilling condition for this given propeller, meaning that it generates virtually no torque on the shaft and thus cannot help drive the generator to save fuel.

4.3 Fuel Consumption

The main mission to be analyzed was chosen to be one with a 900 *kg* payload, equivalent to 9 passengers, meaning that the fuel mass carried by the conventional Caravan was of 843 *kg*. The mission was set up by a Climb-out segment followed by a Climb, Cruise, Descent and Approach segments. The cruise time to fulfill this mission was found to be 4.18 hours, resulting on a range of 761 *nmi*. The fuel required to fly this mission plus a 101 *nmi* alternate was simulated at 841.9 *kg*, consuming all the carried fuel.
Figure 11 shows the mission profile without the reserves. Both the original and the modified aircraft were flown in this mission and the result was that the smaller wing aircraft burned 727.5 *kg* of fuel against 747.6 by the conventional, a 2.7% reduction. This fuel savings come from the reduced parasitic drag throughout the mission from a smaller wing, at the cost of reduced payload at only 530 kg, or approximately 4 passengers less because of the extra wing and propulsive system weight.
Another interesting comparison would be how those aircraft fare when carrying the same payload on the same mission. To carry the same as the conventional Caravan, the DEP aircraft has to carry less fuel and therefore, fly a shorter range, calculated at 383 *nmi* (plus 101 *nmi* for the reserve mission which is not simulated). The profile is the same shown on the previous picture, albeit with a shorter cruise segment.

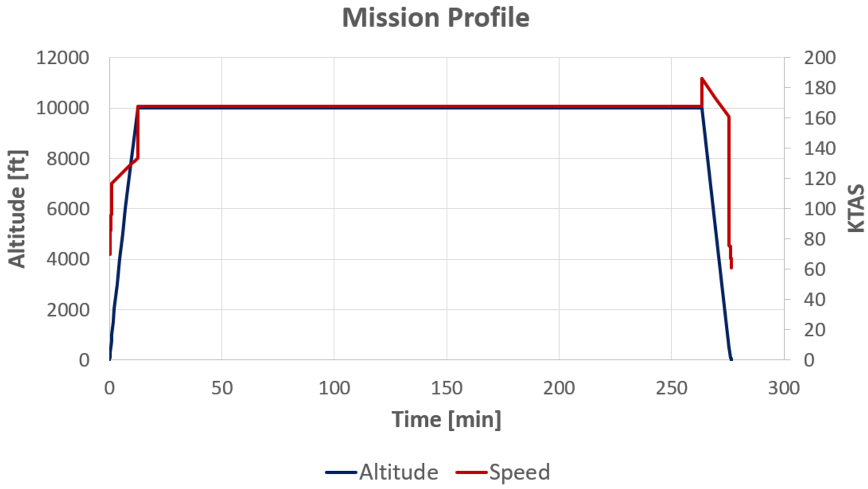

Figure 11 – Long operational mission profile.

Both aircraft were flown on this shorter range, in this case the conventional one taking off at 3600 *kg* (against 3978 *kg* on the DEP one), carrying less fuel (both carrying 474 kg), and the result is that in this case both aircraft consumed virtually the same amount of fuel at 375.9 kg for the conventional and 375.8 kg for the smaller wing aircraft.
Figure 12 gives some insight on this result, showing the engine shaft power and fuel flow difference between both aircraft. While the conventional, lighter one, requires less power and fuel during the climb segments, the fuel flow for both of them is almost the same during cruise where the majority of time is spent. After cruise, on the descent, the DEP aircraft is actually more efficient and consumes less fuel than its counterpart.

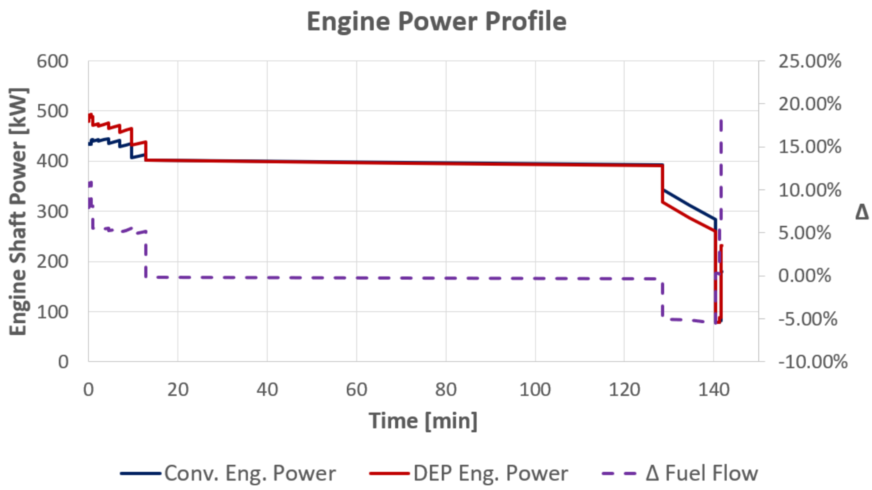

Figure 12 – Short operational mission power and consumption.

To better understand this behavior, Figure 13 shows the drag difference between the DEP and conventional aircraft on all flight phases. The extra weight results in more induced drag on the DEP, while the parasitic drag is always smaller due to the reduced wing. However, even though the induced drag difference seems more relevant, it is greatly influenced by speed (which changes the C_L) so, at lower speeds, the total drag is actually higher for the DEP aircraft but as the speed increases and lift coefficient decreases, the total drag difference drops and at cruise the drag increase due to extra weight is completely nullified by the reduced parasitic drag on the smaller wing.
Table 3 summarizes the analyses, and it shows that even though the distributed electric propulsion and smaller wing does bring aerodynamic gains and benefits for the aircraft, the weight penalty is

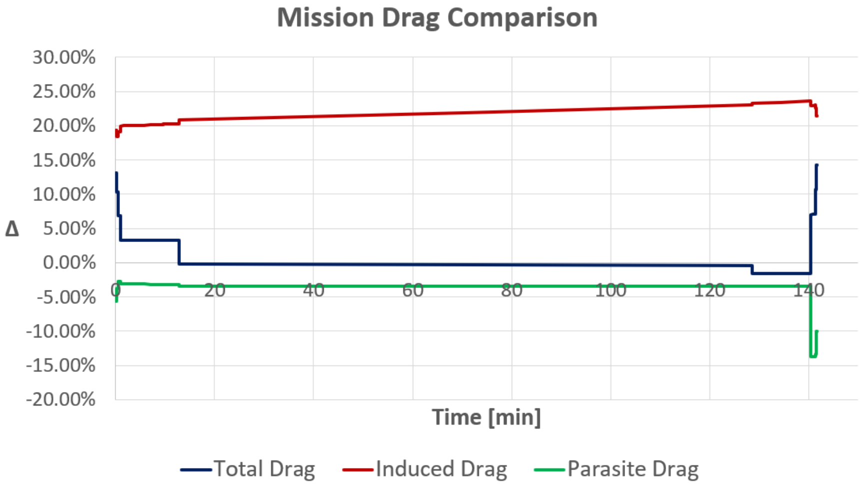

Figure 13 – Short operational mission drag.

too high, limiting payload or range and effectively negating the achieved gains. In the end, flying a conventional aircraft at a lighter weight can achieve the same fuel savings with much less effort.

		Analysis 1	Analysis 2	Analysis 3
Main Mission Range [nmi]		761	761	383
Alternate Flown [nmi]		101	0	0
Takeoff Weight [kg]	**Conventional**	3969	3969	3600
	DEP	3969	3969	3969
Payload [kg]	**Conventional**	900	900	530
	DEP	530	530	530
Carried Fuel [kg]	**Conventional**	843	843	474
	DEP	843	843	474
Consumed Fuel [kg]	**Conventional**	841.9	747.6	375.9
	DEP	819.9	727.5	375.8

Table 3 – Fuel consumption analyses summary.

5. Conclusion

This work expands on results previously published [8] where a Cessna Grand Caravan model was implemented and modified to include the effects of high-lift propellers through the use of distributed electric propulsion. An exploration of the design space was made in terms of wing area and propeller dynamic pressure ratio to observe the effects on the propulsive system sizing, weight, and ultimately mission fuel consumption.

The amount of power required to generate enough lift to reduce wing area in great proportions were found to be very high, even surpassing the total engine available power depending on the wing area reduction. This resulted in significant increase in weight due to the DEP electrical components besides an weight increase on the wing due to higher the aspect ratio.

For a chosen design point of 28% of wing area reduction the DEP aircraft was simulated on different missions and compared to the conventional version. The critical points mission showed that the design accomplishes its goal of increasing the $C_{L_{max}}$ enough so that the reduced wing doesn't stall, however it is only needed in very slow flight speed segments. On the final approach, when the aircraft is at very low speeds and descending, the nose propeller has to generate drag given the high thrust generated by the high-lift propellers.

On a regular mission the added weigh results in a reduction of 4 pax worth of payload capabilities for a fuel reduction of only 2.7%. If payload is kept the same the extra weight accounts for a range loss of roughly 380 nm and, when compared to the conventional aircraft, presents no fuel savings at all.

In the end, given the less-than-expected aerodynamic gains and operational limitations previously published [8] coupled with the weight increase of the new components the result is that there are virtually no gains for the aircraft or operation.

6. Contact Author Email Address

mailto: gallani.murilo@gmail.com

7. Copyright Statement

References

[1] Kim H D, Perry A T and Ansell P J. A Review of Distributed Electric Propulsion Concepts for Air Vehicle Technology. *AIAA/IEEE Electric Aircraft Technologies Symposium*, Cincinatti, OH, 2018.

[2] Jansen R, Bowman C, Jankovsky A, Dyson R and Felder J. Overview of NASA Electrified Aircraft Propulsion (EAP) Research for Large Subsonic Transports. *AIAA/SAE/ASEE Joint Propulsion Conference*, Atlanta, GA, 2017.

[3] Pornet C and Isikveren A T. Conceptual design of hybrid-electric transport aircraft. *Progress in Aerospace Sciences*, Vol. 79, pp 114-135, 2015.

[4] Gesell H, Wolters F and Plohr M. System analysis of turbo-electric and hybrid-electric propulsion systems on a regional aircraft. *The Aeronautical Journal*, Vol. 123, No. 1268, pp 1602-1617, 2019.

[5] Lenssen R H. *Series Hybrid Electric Aircraft - Comparing the Well-to-Propeller efficiency with a conventional propeller aircraft*. M. Sc in Aerospace Engineering, Delft University of Technology, 2016.

[6] Dean T, Wroblewsy G E and Ansell P J. Mission Analysis and Component-Level Sensitivity Study of Hybrid-Electric General Aviation Propulsion Systems. *AIAA Aerospace Sciences Meeting*, Kisimee, FL, 2018.

[7] NAS. *Commercial Aircraft Propulsion and Energy Systems Research - Reducing Global Carbon Emissions*. The National Academic Press, 2016.

[8] Gallani M A, Góes L C S, Nerosky L A R. Effects of Distributed Electric Propulsion on the Performance of a General Aviation Aircraft. *AIAA Propulsion and Energy Forum*, 2020.

[9] Stoll A M, Bevirt J, Moore M D, Fredericks W J and Borer N K. Drag Reduction Through Distributed Electric Propulsion. *AIAA Aviation Technology, Integration, and Operations Conference*, Atlanta, GA, 2014.

[10] Stoll A M. Comparison of CFD and Experimental Results of the LEAPTech Distributed Electric Propulsion Blown Wing. *AIAA Aviation Technology, Integration, and Operations Conference*, Dallas, TX, 2015.

[11] Stoll A M and Mikic G V. Design Studies of Thin-Haul Commuter Aircraft with Distributed Electric Propulsion. *AIAA Aviation Technology, Integration, and Operations Conference*, Washington, DC, 2016.

[12] Borer N K, Patterson M D, Vicken M D, Moore M D, Clarke S, Redifer M E, Christie R J, Stoll A M, Dubois A, Bevirt J, Gibson A R, Foster T J and Osterkamp P J. Design and Performance of the NASA SCEPTOR Distributed Electric Propulsion Flight Demonstrator. *AIAA Aviation Technology, Integration, and Operations Conference*, Washington, DC, 2016.

[13] Patterson M D. *Conceptual Design of High-Lift Propeller Systems for Small Electric Aircraft*. PhD in Aerospace Engineering, Georgia Institute of Technology School of Aerospace Engineering, 2016.

[14] Lucaczyk T W, Wendorff A D, Cononno M, Economon T D, Alonso J J, Orra T H and Ilario C. SUAVE - An Open-Source Environment for Multi-Fidelity Conceptual Vehicle Design. *AIAA/ISSMO Multidisciplinary Analysis and Optimization Conference*, Dallas, TX, 2015.

[15] Gallani M A. *Analysis of the Application of Distributed Propulsion on a Turboelectric General Aviation Aircraft*. M. Eng. in Aeronautical Engineering, Instituto Tecnológico de Aeronáutica, 2019.

[16] Cessna Aircraft Company. *Information Manual Grand Caravan*. Wichita, 2018.